Laser Propulsion using a Molecular Absorber

V.P. Chiravalle*, R.B. Miles†, and E.Y. Choueiri‡
MAE Dept.
Princeton University
Princeton, New Jersey 08544

AIAA-98-3932§

Abstract

This paper explores the concept of laser propulsion using a molecular absorber. Unlike the conventional approach of using a laser sustained plasma to heat a propellant, molecular absorption of laser energy makes it possible to avoid the frozen flow losses associated with the high temperature and complex chemistry of a plasma. The molecular absorption concept is developed by exploring several thermodynamic pathways for energy addition in the supersonic regime, which are visualized as curves in H-K coordinates. The case of an isothermal expansion is studied in depth. The absorption physics of a promising molecular absorber, SF_6, is described at arbitrary laser beam intensities using a two-temperature nonequilibrium model, which is then applied to calculate the required length of the supersonic energy addition region in a laser rocket nozzle.

1 Introduction

As high-power laser technology continues to mature the possibility of using a laser to generate rocket thrust for propulsion applications grows more feasible. The laser propulsion concept was first introduced by Kantrowitz[1] , more than twenty five years ago, and was experimentally demonstrated by Krier et. al.[2] and by Myrabo[3] . As with any thermal propulsion system, the efficiency of conversion of laser beam energy into the kinetic energy of propellant gas is a critical figure of merit. In addressing laser thruster performance it is useful to consider both the absorption efficiency as well as the the propulsion efficiency. In the context of laser thrusters, the propulsion efficiency is a measure of how much absorbed energy appears as kinetic energy of the propellant at the nozzle exit.

The established approach for achieving energy conversion is to create a laser sustained plasma (LSP) in the flowing propellant. The plasma is localized near the focal point of a laser beam, and laser energy is absorbed through the electron inverse bremsstralung process. As the propellant gas flows through and around the stationary plasma high bulk temperatures are sustained which can be in excess of 10,000 K in gases such as argon. Stable LSPs were created and observed by Keefer et. al.[4], who report absorption efficiencies as high as 86 %. Several attempts have been made to visualize the physical interactions occurring in laboratory LSPs using two dimensional numerical simulations[5, 6]. Although the coupling of laser energy to a plasma has been found to be quite high, the overall propulsion efficiency is not as good. There are several processes that degrade the efficiency. In general, plasma radiation is a significant contributor, and in the case of molecular propellants such as hydrogen, dissociative frozen flow losses are also important. The equilibrium fraction of dissociated hydrogen is known to vary exponentially with temperature, and the reduction of frozen flow losses in hydrogen thermal thrusters necessitates finding a way to add significant amounts of energy without completely dissociating the propellant. The dissociation fraction of hydrogen for various temperatures and densities is shown in Fig. 1.

*Graduate Student, Mechanical & Aerospace Engineering, AIAA

†Professor, Mechanical & Aerospace Engineering, Associate Fellow AIAA

‡Assistant Professor, Mechanical & Aerospace Engineering, Senior Member AIAA

§This work was supported by an AASERT award from the Air Force Office of Scientific Research (AFOSR).

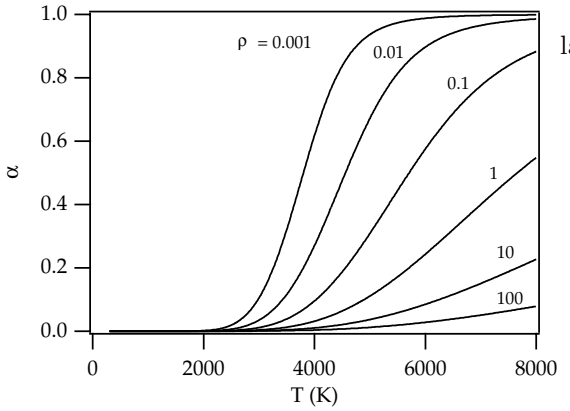

Figure 1: The calculated equilibrium dissociation fraction of H_2 is presented above, as a function of temperature and density.

A different approach for energy addition, one that does not utilize a plasma, is the molecular absorption of radiation in the supersonic regime. Adding energy using a molecular absorber involves the excitation of an internal mode such as rotation or vibration of a seed molecule, the seed molecule subsequently transfers its energy to the propellant gas by relaxation collisions. The molecular absorption approach for laser propulsion was previously identified by Caledonia et. al.[7] in 1975. More recently, molecular absorption has been considered as an energy addition mechanism in the supersonic region for a proposed atmospheric, hypersonic wind tunnel and has been the focus of an ongoing research effort[8, 9].

The central issues with this approach involve the choice of the thermodynamic path over which energy is added and the choice of the seed molecule, with its associated set of physical parameters. Fig. 2 shows that with a molecular absorber it is possible to extend the energy addition region throughout the nozzle rather than concentrating all the energy in the plenum, the way it is done in conventional propulsion systems. The goal of this paper is to explore relatively simple energy pathways, such as constant temperature expansion to gain insight into the more complicated cases that may be of use to laser propulsion. The interaction between the seeded propellant mixture and the laser beam is described in general terms, using a familiar quasi-one dimensional model. It is understood that this approach is useful in a restricted sense, and is intended as a starting point for more robust numerical simulations. This formalism is then applied using absorption data for SF_6 to calculate the length of the energy addition region in a laser thruster with molecular absorption.

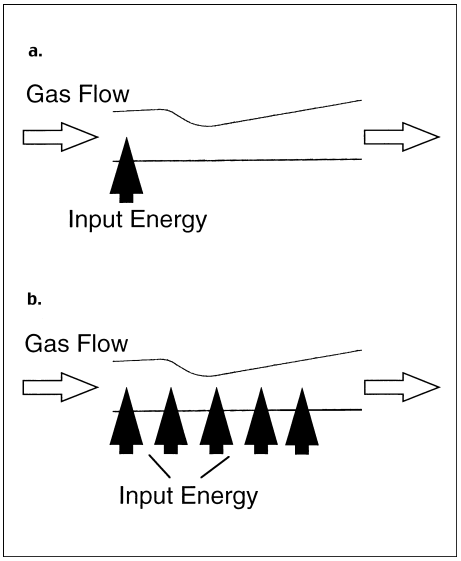

Figure 2: Illustrated above are the laser rocket propulsion concepts discussed in this paper: a: Energy addition using a laser sustained plasma in the plenum region. b: Energy addition in the supersonic region using a molecular absorber.

2 Fluid Model for Energy Addition

Within the constraints of one dimensional theory, the physics of an absorbing fluid in steady state is expressed by the fluid conservation equations,

$$\frac{1}{A}\frac{dA}{dx} + \frac{1}{\rho}\frac{d\rho}{dx} + \frac{1}{u}\frac{du}{dx} = 0 \quad (1)$$

$$\frac{dP}{dx} + \rho u\frac{du}{dx} = 0 \quad (2)$$

$$c_p\frac{dT}{dx} + u\frac{du}{dx} = \frac{dT_0}{dx}. \quad (3)$$

T_0 is the total temperature of the fluid and $\frac{dT_0}{dx} = \kappa\frac{dP_w}{dx}$. P_w is the laser power which is assumed to be uniform across the beam cross section. It is assumed also that the gas is ideal and perfect i.e. with $P = \rho RT$ and constant c_p.

The absorption coefficient, κ, is in general a function of the gas thermodynamic variables T and ρ and the laser intensity, I. There are more variables in

this system than equations relating them. When the nozzle area, A, is specified everywhere and when the laser power incident to the energy addition region, P_{w0}, is known, the above equations uniquely determine the thermodynamic and mechanical state of a gas with a given set of initial conditions.

It is well known that if a transformation is performed, expressing all quantities in terms of the optical length, $\tau = \int \kappa dx$, the conservation equations can be solved without reference to the properties of the absorbing species[7, 10]. The solution in physical space is recovered, for a chosen absorber, by reversing the transformation. There are limitations to the effectiveness of this approach since the radius of the nozzle is now a function of τ. Choosing $A(\tau)$ to give a specific shape in physical space is not intuitively obvious.

This difficulty can be removed, if instead of constraining the nozzle to have a given profile in space, an additional relation among the fluid variables is specified. The enlarged system of equations is solved with A as a variable. In this way nozzle profiles are determined to satisfy thermodynamic constraints. The additional relation can be chosen as

$$\frac{dH}{dK} = \chi, \tag{4}$$

with $K = \frac{u^2}{2}$ and $H = c_p T$. Going a step further, all the variables that describe the fluid, A, T_0, ρ, T, and u, can be written in terms of M^2, γ and χ,

$$\begin{aligned}
\frac{1}{A}\frac{dA}{d\tau} &= \frac{((\gamma-1)\chi+\gamma)M^2-1}{2-\chi(\gamma-1)M^2}\frac{dM^2}{d\tau},\\
\frac{1}{T_0}\frac{dT_0}{d\tau} &= \frac{(\gamma-1)(\chi+1)}{(1+\frac{\gamma-1}{2}M^2)(1-\chi(\gamma-1)M^2)}\frac{dM^2}{d\tau},\\
\frac{1}{\rho}\frac{d\rho}{d\tau} &= -\frac{(\gamma-1)\chi+\gamma}{2-\chi(\gamma-1)M^2}\frac{dM^2}{d\tau},\\
\frac{1}{T}\frac{dT}{d\tau} &= \frac{\chi(\gamma-1)}{2-\chi(\gamma-1)M^2}\frac{dM^2}{d\tau},\\
\frac{1}{u}\frac{du}{d\tau} &= \frac{1}{M^2(2-\chi(\gamma-1)M^2)}\frac{dM^2}{d\tau},
\end{aligned} \tag{5}$$

where for the moment χ is an unspecified function of M^2. The above equations trace curves in a five dimensional space parametized by M^2.

Another way to visualize the above relations is to look at their trajectories in H-K coordinates[11] . In the H-K plane each horizontal line, $\chi = 0$, corresponds to a constant temperature process and each vertical line, $\chi \to \infty$, corresponds to a constant pressure process. Three other basic cases are heat transfer with constant area, adiabatic, isentropic expansion and constant Mach number heating of the gas. The appropriate χ functions for these three cases are given below

$$\chi = (1-\gamma M^2)/M^2(\gamma-1), \tag{6}$$
$$\chi = -1, \tag{7}$$
$$\chi = 2/(\gamma-1)M^2, \tag{8}$$

where Eq. 6 refers to the constant area heat transfer case, Eq. 7 refers to the adiabatic, isentropic expansion case and Eq. 8 refers to the constant Mach number case. The example cases just discussed are illustrated in Fig. 3, and do not exhaust the set of possible curves in H-K space. Any function $\chi(M^2)$ defines a path for the thermodynamic and mechanical parameters of the fluid to traverse. The task with regard to laser propulsion is to identify the χ function or set of functions which achieve a required exhaust velocity, while having desirable characteristics in terms of efficiency of laser energy addition and nozzle size.

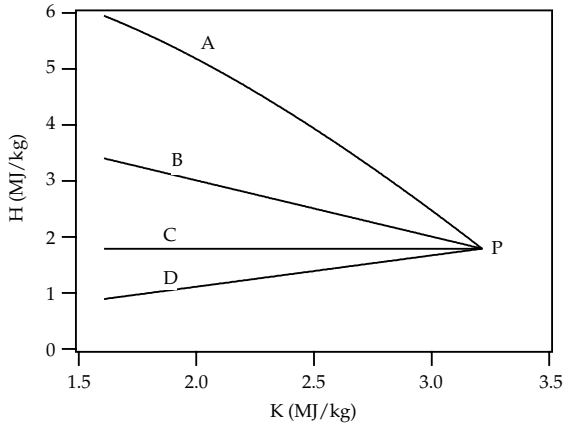

Figure 3: This figure shows the H-K coordinates of four trajectories in the supersonic regime that intersect at point P. The conditions at P represent a mixture of H_2 with 2 % SF_6 at T=300 K with M=3.0. (A) refers to a cooling process with constant area, (B) refers to an adiabatic, isentropic expansion process, (C) refers to an isothermal expansion process and (D) refers to a heating process at constant Mach number.

An attempt is made in the following sections to do this by solving the case of $\chi = 0$, isothermal flow, using a realistic model of a molecular absorber, SF_6. An isothermal energy pathway was selected for the

examples in this work to ensure that the temperature would remain below the dissociation limit everywhere in the nozzle. The solution is obtained for the fluid variables in τ-space first, then the results are transformed back into physical space by computing the SF_6 absorption coefficient at each point in the nozzle. SF_6 was chosen because of its exceptionally high absorption coefficient at 10.6μm, the wavelength of commercial CO_2 lasers. As discussed later the required SF_6 absorption data exist in a narrow temperature range around 300 K, and for this reason 300 K was used in all the example cases computed here.

3 Study Case: Isothermal Expansion

Consider an isothermal expansion taking place in the supersonic region of a laser thruster. The laser enters at the nozzle exit and propagates in the direction of the throat, as seen in Fig. 4.

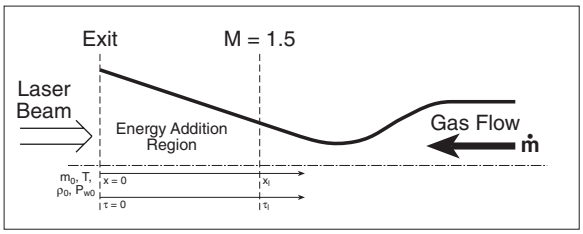

Figure 4: This figure shows the orientation of the laser beam propagation relative to the fluid flow in the examples considered in this study. The non-dimensional optical length, τ, and the physical axial length are measured relative to the nozzle exit where the laser beam enters and the fluid conditions are specified.

The energy addition term of Eq. 3 is related to the power extracted from the laser beam. In τ-space the equation describing the evolution of the beam power can be written as

$$\frac{dP_w}{d\tau} = -P_w. \tag{9}$$

The solution is an exponential function of τ. τ is measured relative to the nozzle exit, and the direction of increasing τ corresponds, in physical space, to marching upstream toward the throat, Fig. 4. With this expression for P_w and the isothermal condition, analytic solutions for M^2 and ρ can be obtained as a functions of τ and of the conditions at the nozzle exit. These are used to compute the flow properties at each section of the nozzle and are given below

$$M^2 = M_0^2 + \frac{2\Gamma}{\gamma}\left[1 - \exp -\tau\right], \tag{10}$$

$$\rho = \rho_0 \exp \Gamma \left[1 - \exp -\tau\right]. \tag{11}$$

The non-dimensional parameter Γ has the form $\Gamma = P_{w0}/\dot{m}RT$ and in physical terms it is proportional to the ratio of incident laser beam power to flow enthalpy.

4 SF_6 Absorption Physics

Gaseous SF_6 is a strong absorber of infrared radiation at the $C0_2$ laser wavelength. A spherical top molecule, SF_6 has six fundamental vibrational modes, one of these, designated by the ν_3 quantum number, corresponds to an infrared active band. In addition to vibrational motion the SF_6 molecule also has rotational energy components, described collectively by the quantum number J. Let N_1 be the number density of SF_6 in a state with none of its vibrational modes excited and with a rotational quantum number, J_1; let N_2 be the corresponding number density for a state with $\nu_3 = 1$ and with rotational quantum number J_2. The absorption coefficient can be expressed as a function of N_1 and N_2 according to the equation below,

$$\kappa = \sigma(N_1 - \frac{g_1}{g_2}N_2). \tag{12}$$

Based on the measurements by Anderson [12] in pure SF_6 at 100 torr and 300 K, the value of κ is 3500 m^{-1}. Computing N_1 and N_2 at these conditions, the absorption cross section, σ, can be determined from the experimental value for the absorption coefficient, κ.

To understand the effect of laser intensity on κ, it is necessary to explore the physics contained in the N_1 and N_2 terms. At equilibrium conditions N_2 and N_1 are determined by the Boltzmann relation and depend entirely on the thermodynamic temperature. Situations may arise when the translational and vibrational modes of the fluid become uncoupled, for instance when a fluid is perturbed by a tightly focused laser or when a shock wave passes through the fluid. In such a case N_1 and N_2 are described in terms of two temperatures, a translational temperature, T, and a vibrational temperature, T_{vib}. Energy transfer from one mode of vibration to another occurs on a short time scale relative to energy transfer to a translational mode. The evolution of the fluid vibrational

energy is described by a conservation equation which in steady state appears as

$$\dot{m}\frac{de_{vib}}{dx} = \frac{\rho A(e^*_{vib} - e_{vib})}{\beta} + \kappa P_w. \qquad (13)$$

β, the characteristic time for vibrational relaxation, was measured for pure SF_6 by Burak et. al.[13] and was found to be 140 μsec torr. This value was adopted in this work, although it should be noted that for laser propulsion the interest is in SF_6-gas mixtures, not in pure SF_6, whose molecular mass is considerably greater than that of useful propellants like hydrogen. For this reason one would expect the relaxation time to be shorter for an SF_6-H_2 mixture than for pure SF_6. Eq. 13 can be transformed from physical space into τ-space in the same way as the other fluid conservation equations. When this is done a coefficient, $1/u\kappa$ appears, which is the characteristic flow residence time. The flow residence time is the time required for the fluid to travel a distance equal to the distance over which the laser beam intensity drops by a factor of $1/e$. de_{vib}/dx can be neglected in Eq. 13 when two criteria are met simultaneously, the flow residence time, σ, is much longer than the vibrational relaxation relaxation time, β, and the difference between the vibrational energy that the flow would have at equilibrium, e^*_{vib}, and the flow vibrational energy, e_{vib}, is the same order of magnitude as e_{vib}. e_{vib} is a function of T_{vib} and e^*_{vib} is a function of T. The conditions for neglecting de_{vib}/dx are summarized below,

$$\sigma \gg \beta,$$
$$e^*_{vib} - e_{vib} \sim e_{vib}. \qquad (14)$$

The functional forms of the terms, N_1, N_2, e_{vib} and e^*_{vib}, are given in Ref. [12].

A two-temperature approach was put forth by Anderson[12] to treat saturation absorption in SF_6 at high laser intensities. The model presented in that work is used here to compute the SF_6 absorption coefficient and is strictly valid at room temperature, 300 K, where absorption data was collected. The present implementation of the model differs from the one used by Anderson in one way, only absorption from the ground state is considered here. The original model considered absorption from both the ground state and an excited state. The present model is more conservative in the sense that at high laser beam intensities the absorption coefficient is less because absorption by excited states is not considered.

5 Results for a Supersonic Isothermal Expansion with SF_6 as an Absorber

To assess the potential of laser propulsion using a molecular absorber it is necessary to get a rough answer to some basic questions regarding how much energy can be deposited in the supersonic region of an expanding nozzle flow, whether the expansion can begin at a low enough temperature to avoid hydrogen dissociation and if the nozzle size in such a system is so large as to be impractical. As discussed in the previous sections, one possible way of introducing the laser into the supersonic energy addition region is to direct the beam from downstream through the nozzle exit. For nozzles where the supersonic expansion ratio is sufficiently gradual the one dimensional theory developed in this paper is not a bad approximation. This is true of the nozzles considered in this section.

The fluid conditions and laser beam power are specified at the nozzle exit. Using Eq. 10 and Eq. 11 the conditions at all other points upstream of the exit in the energy addition region are uniquely determined. The nozzle exit conditions were chosen to be realistic values for an expanded supersonic flow, such as $M_0 = 3.0$ and $\rho_0 = 0.001$ kg/m^3. T was set to 300 K for reasons discussed earlier and the mass flow rate was selected as 10 g/sec to keep the required nozzle exit diameter in the 5-10 cm range. The computation marched forward toward the throat from the exit, and was concluded when the flow achieved $M = 1.5$. The propellant mixture consisted of H_2 with an SF_6 concentration of 2 %. The laser beam power was allowed to vary for each run. For a given run, the first step was to find the point in τ-space where $M = 1.5$, this was accomplished using Eq. 10. Then for all points in the energy addition region, Eq. 13 was solved numerically for T_{vib} assuming, $de_{vib}/dx \approx 0$, and the absorption coefficient was calculated using Eq. 12. Knowing κ at all points in the energy addition region, the nozzle radial profile and all the fluid conditions were determined as functions of axial length.

Twenty two runs were made with the nozzle exit conditions discussed above. For each run the laser beam power was increased. For a given value of laser power, the non-dimensional optical length at the position where $M = 1.5$, denoted τ_L, was calculated and the corresponding position, x_L, was then determined. Fig. 5 shows how x_L varies with laser power. The laser beam power is non-dimensionalized in terms of

$\dot{m}RT$. The absorption coefficient, κ, at the point where $M = 1.5$, is used to non-dimensionalize x_L. The largest nozzle size of 0.72 m occurs when $\Gamma = 5.0$. This case is also the case where most of the laser beam power is absorbed in the supersonic region. The fraction of laser beam power absorbed in the supersonic region to the incident laser beam power is shown in Fig. 7. As the laser beam power is increased two trends occur, the required nozzle size in the supersonic energy addition region decreases and the fraction of absorbed power decreases, i.e. more of the laser power passes through the intended energy addition region into the throat region. Looking at Fig. 5 and Fig. 7, it is evident that there is a limit for Γ, which can be found by solving Eq. 10 for Γ as $\tau \to \infty$. For the specified Mach number at the nozzle exit, $M_0 = 3.0$, the limit is $\Gamma = 4.72$. The laser beam power corresponding to $\Gamma = 4.72$ is 24 kW and represents the minimum amount of input power, $\dot{m}c_p dT_0/dx$, required to satisfy the isothermal condition from $M = 1.5$ to $M = 3.0$. Laser beams of greater power propagate through the supersonic energy addition region without being completely attenuated, i.e. $\eta < 1$.

Among the cases computed the results for Γ of 5.63, 9.67 and 23.12 are presented. The ratio of flow residence time to vibrational relaxation time is plotted in Fig. 8, and it is seen that σ is at least an order of magnitude larger than β. The ratio of vibrational temperature to translational temperature is given in Fig. 6, and is everywhere greater than 1. It is evident, therefore, that the criteria for neglecting de_{vib}/dx are satisfied in the cases considered. As the laser beam power is increased T_{vib} increases, raising N_2 and lowering N_1. The net effect is to decrease κ. The computed nozzle profile for the case with $\Gamma = 5.63$ is shown in Fig. 9. At the nozzle exit the radius is 3.5 cm. The right most point on the graph corresponds to the $M = 1.5$ point, where the radius is 0.47 cm. The total length is 68 cm with an area expansion ratio of 56.

6 Conclusions

The concept of laser propulsion using a molecular absorber was studied by choosing a simple isothermal pathway for energy addition, and by implementing a realistic model of SF_6 absorption. The results indicate that significant amounts of energy can be deposited in the supersonic region without paying too unreasonable a penalty in terms of nozzle length. Although one energy addition pathway was explored in depth in this paper, other traditional cases such as constant Mach number energy addition, and other less familiar χ functions should also be studied. To do so with SF_6, however requires additional absorption data to describe how σ varies in the high T regime, since no data of this type exist today. The I_{sp} of the example cases studied here was 250 *sec*, operation at a higher temperature, although not high enough to cause dissociation, would open the door to a higher specific impulse.

References

[1] A. Kantrowitz. Propulsion to orbit by ground-based lasers. *Astronautics and Aeronautics*, 10:74–76, 1972.

[2] H. Krier, J. Black, and R.J. Glumb. Laser propulsion 10 kw thruster test program results. *Journal of Propulsion and Power*, 11:1307–1316, 1995.

[3] L.N. Myrabo, D.G. Messitt, and F.B. Mead Jr. Ground and flight tests of a laser propelled vehicle. In *AIAA* 36^{th} *Aerospace Sciences Meeting*, Reno, NV, January 1998. AIAA 98-1001.

[4] R. Welle, D. Keefer, and C. Peters. Laser-sustained plasmas in forced argon convective flow, part 1: Experimental studies. *AIAA Journal*, 25:1093–1099, 1987.

[5] S. Jeng and D. Keefer. Theoretical investigation of laser sustained argon plasmas. *Journal of Applied Physics*, 60:2272–2279, 1986.

[6] A. Mertogul and H. Krier. Two-temperature modeling of laser sustained hydrogen plasmas. *Journal of Thermophysics and Heat Transfer*, 8:781–790, 1994.

[7] G.E. Caledonia, P.K.S. Wu, and A. N. Pirri. Radiant energy absorption studies for laser propulsion. Final Report NASA-CR-134809, NASA Lewis Research Center, 1975.

[8] R.B. Miles, G.L.Brown, W.R. Lempert, R. Yetter, G.J. Williams Jr., S.M.Bogdonoff, D. Natelson, and J.R. Guest. Radiatively driven hypersonic wind tunnel. *AIAA Journal*, 33:1463–1469, 1995.

[9] R.B. Miles and G.L. Brown. Energy addition mechanisms for radiatively-driven wind tunnel: Predictions & experiments. In *AIAA* 29^{th}

Plasmadynamics and Lasers Conference, Albuquerque, NM, June 1998. AIAA 98-2748.

[10] W.G. Vincenti and C.H. Kruger. *Introduction to Physical Gas Dynamics*. John Wiley & Sons, 1965.

[11] D.T. Pratt and W.H. Heiser. Isolator-combustor interaction in a dual-mode scramjet. In *AIAA* 31^{th} *Aerospace Sciences Meeting*, Reno, NV, January 1993. AIAA 93-0358.

[12] J.D. Anderson Jr. and J.L. Wagner. CO_2 laser radiation absorption in SF_6-air boundary layers. In *AIAA* 11^{th} *Aerospace Sciences Meeting*, Washington, D.C., January 1973. AIAA 73-262.

[13] J.I. Steinfeld, I. Burak, D.G. Sutton, and A.V. Nowak. Infrared double resonance in sulfur hexafluoride. *Journal of Chemical Physics*, 52:5421–5434, 1969.

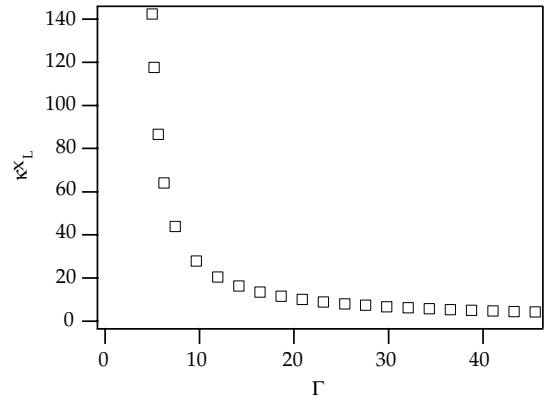

Figure 5: This figure shows the calculated nozzle length for supersonic energy addition versus the laser beam power incident at the nozzle exit. 22 cases were considered. The left most point corresponds to having $\Gamma = 5.0$.

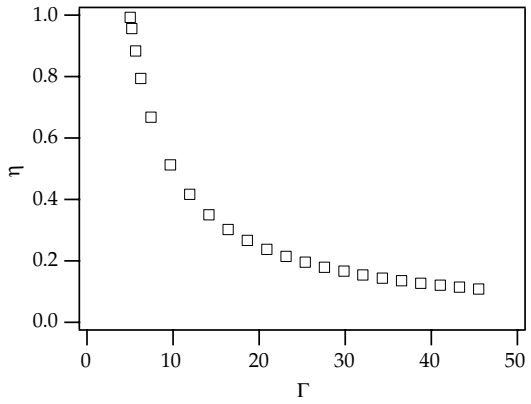

Figure 7: This figure shows the fraction of laser beam power absorbed in the supersonic region, η, versus the laser beam power incident at the nozzle exit.

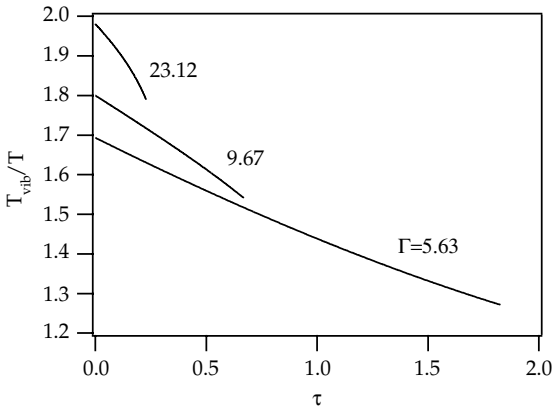

Figure 6: The ratio of SF_6 vibrational temperature to the fluid translation temperature, 300 K, is displayed as a function of the non-dimensional optical depth, τ.

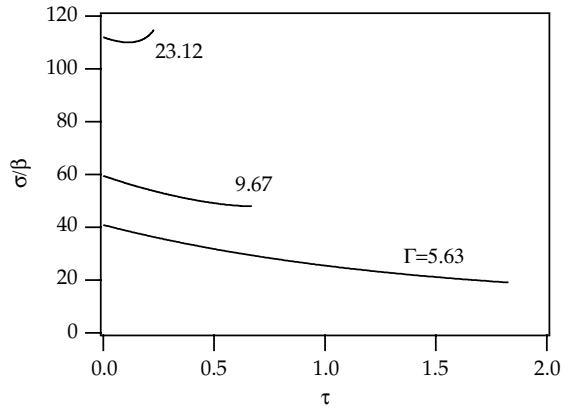

Figure 8: The ratio of the characteristic flow residence time to the vibrational relaxation time of SF_6 is displayed as a function of the non-dimensional optical length.

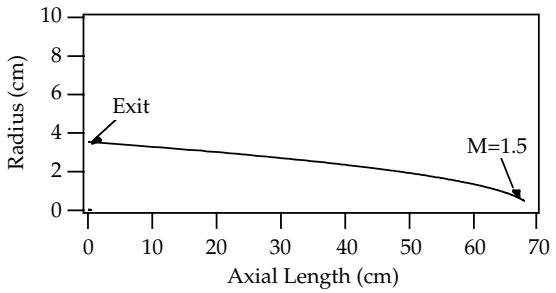

Figure 9: This figure shows the computed nozzle profile, nozzle radius versus axial length, for supersonic energy addition with $\Gamma = 5.63$.